CLIMATE CHANGE, GROWTH, AND CALIFORNIA WILDFIRE

A Paper From:
California Climate Change Center

Prepared By:
A. L. Westerling, B. P. Bryant, H. K. Preisler, T. P. Holmes, H. G. Hidalgo, T. Das, and S. R. Shrestha

DISCLAIMER

Arnold Schwarzenegger, *Governor*

FINAL PAPER

Acknowledgments

Preface

The California Energy Commission's Public Interest Energy Research (PIER) Program supports public interest energy research and development that will help improve the quality of life in California by bringing environmentally safe, affordable, and reliable energy services and products to the marketplace.

The PIER Program conducts public interest research, development, and demonstration (RD&D) projects to benefit California's electricity and natural gas ratepayers. The PIER Program strives to conduct the most promising public interest energy research by partnering with RD&D entities, including individuals, businesses, utilities, and public or private research institutions.

PIER funding efforts focus on the following RD&D program areas:

- Buildings End-Use Energy Efficiency
- Energy-Related Environmental Research
- Energy Systems Integration
- Environmentally Preferred Advanced Generation
- Industrial/Agricultural/Water End-Use Energy Efficiency
- Renewable Energy Technologies
- Transportation

In 2003, the California Energy Commission's PIER Program established the **California Climate Change Center** to document climate change research relevant to the states. This center is a virtual organization with core research activities at Scripps Institution of Oceanography and the University of California, Berkeley, complemented by efforts at other research institutions. Priority research areas defined in PIER's five-year Climate Change Research Plan are: monitoring, analysis, and modeling of climate; analysis of options to reduce greenhouse gas emissions; assessment of physical impacts and of adaptation strategies; and analysis of the economic consequences of both climate change impacts and the efforts designed to reduce emissions.

The California Climate Change Center Report Series details ongoing center-sponsored research. As interim project results, the information contained in these reports may change; authors should be contacted for the most recent project results. By providing ready access to this timely research, the center seeks to inform the public and expand dissemination of climate change information, thereby leveraging collaborative efforts and increasing the benefits of this research to California's citizens, environment, and economy.

For more information on the PIER Program, please visit the Energy Commission's website www.energy.ca.gov/pier/ or contract the Energy Commission at (916) 654-5164.

Table of Contents

List of Figures

List of Tables

Abstract

Large wildfire occurrence and burned area are modeled using hydroclimate and landsurface characteristics under a range of future climate and development scenarios. The range of uncertainty for future wildfire regimes is analyzed over two emissions pathways (the *Special Report on Emissions Scenarios* [SRES] A2 and B1 scenarios); three global climate models (Centre National de Recherches Météorologiques CM3, Geophysical Fluid Dynamics Laboratory CM21 and National Center for Atmospheric Research PCM2); a mid-range scenario for future population growth and development footprint; two model specifications related to the uncertainty over the speed and timing with which vegetation characteristics will shift their spatial distributions in response to trends in climate and disturbance; and two thresholds for defining the wildland-urban interface relative to housing density. Results were assessed for three 30-year time periods centered on 2020, 2050, and 2085, relative to a 30-year reference period centered on 1975. Substantial increases in wildfire are anticipated for most scenarios, although the range of outcomes is large and increases with time. The increase in wildfire area burned associated with the higher emissions pathway (SRES A2) is substantial, with increases statewide ranging from 57 percent to 169 percent by 2085, and increases exceeding 100 percent in most of the forest areas of Northern California in *every* SRES A2 scenario by 2085. The spatial patterns associated with increased fire occurrence vary according to the speed with which the distribution of vegetation types shifts on the landscape in response to climate and disturbance, with greater increases in fire area burned tending to occur in coastal southern California, the Monterey Bay area and northern California Coast ranges in scenarios where vegetation types shift more rapidly.

Keywords: Climate, wildfire, ecosystems, hydrology, global change

1.0   Introduction

The climate system interacts with various factors such as soils, topography, available plant species, and sources of ignition to give rise to both natural ecosystems and their fire regimes. Long-term patterns of temperature and precipitation determine the moisture available to grow the vegetation that fuels wildfires (Stephenson 1998). Climatic variability on interannual and shorter scales governs the flammability of these fuels (e.g., Westerling 2003; Heyerdahl et al. 2001; Kipfmueller and Swetnam 2000; Veblen et al. 2000; Swetnam and Betancourt 1998; Balling et al. 1992). Flammability and fire frequency in turn affect the amount and continuity of available fuels. Consequently, long-term trends in climate can have profound implications for the location, frequency, extent, and severity of wildfires and for the character of the ecosystems that support them (Westerling 2008, in press).

Human-induced climatic change may, over a relatively short time period (< 100 years), give rise to climates outside anything experienced in California since the establishment of an industrial civilization currently sustaining a state population that has increased approximately 41,000% since 1850.[1] Changes in wildfire regimes driven by climate change are likely to impact ecosystem services that California citizens rely on, including carbon sequestration in California forests; quality, quantity and timing of water runoff; air quality; wildlife habitat; viewsheds and recreational opportunities. They may also impact the ability of homeowners and federal, state, and local authorities to secure homes in the wildland-urban interface from damage by wildfires (Westerling and Bryant 2008).

In addition to climate change, the continued growth of California's population and the spatial pattern of development that accompanies that growth are likely to directly affect wildfire regimes through their effects on the availability and continuity of fuels and the availability of ignitions. They are also likely to impact both wildfire and property losses due to wildfire through their effects on the extent and value of development in California's wildland-urban interface, both through their effects on the number of structures proximate to wildfire risks and their effects on fire suppression strategies and effectiveness.

The combined effects of climate change and development on California's future large wildfire occurrence and burned area are the focus of the research presented here. Our modeling projects California's fire regimes *as they are currently managed* onto scenarios for future climate, population, and development. The methodology we employ can incorporate the effects of spatial variations in current management strategies on average fire risks. However, the monthly and interannual variations in large wildfire occurrence and burned area that we estimate do not reflect changes in management strategies over time, although our modeling does have the capacity to reflect changes in the effectiveness of current management strategies to the extent that these changes currently tend to correlate with climate and landsurface characteristics. Thus, hypothetical effects of future changes in management in response to the impacts of climate and development on wildfire are not considered in this work.

The metrics we model here—large fire occurrence and burned area—are not the only metrics we would wish to employ to assess the full range of impacts of wildfire on the services and sectors

---

[1] Calculated from population statistics obtained from the U.S. Census online at www.census.gov/.

detailed above. In particular, metrics of fire severity (e.g., the percent of available biomass consumed, characteristics of ecological impacts) would be highly desirable as well. These metrics are likely to change in response to climate, may also be influenced by future management decisions, and are key components for estimating many wildfire impacts due to climate change. The work reported here does not consider changes in fire severity, which are the target of multiple ongoing research efforts. However, in interpreting our results, it would be a mistake to assume a linear correspondence between increased burned area and fire severity. Fire severity is likely increase in some ecosystems and decrease in others alongside increases in burned area. Furthermore, severity might decrease in some ecosystems for reasons that many California residents would find undesirable.

This work extends an analysis by Westerling and Bryant (2008) that considered the effects of climate change on California large wildfire occurrence and wildfire-related damages holding development fixed at the 2000 census. In this analysis we statistically model large (>200 and >8500 hectares [ha]) wildfire occurrence as a product of both future climate scenarios and a future population and development scenario, using nonlinear logistic regression techniques developed for seasonal wildfire forecasting in California and the western United States (Preisler and Westerling 2007). We model the expected burned area using Generalized Pareto Distributions fit to observed wildfires >200 and >8500 ha. We assess a range of outcomes given numerous sources of uncertainty, including three global climate models (GCMs) with different sensitivities of temperature and precipitation to anthropogenic forcing, stochastic differences between GCM runs with respect to the timing of variability in temperature and precipitation, two emissions scenarios, and variations in our wildfire model parameterization that allow for changes in the spatial distribution of vegetation and fire regime types. Our goal is not to determine one most likely outcome, but rather to define a population of plausible outcomes which can be used to assess the robustness of combined adaptation and mitigation policy choices.

2.0   Data and Methods

2.1.   Domain and Resolution

The spatial domain for this analysis is a 1/8-degree lat/long grid (~12 kilometer [km] resolution) bounded by the political boundary for the State of California. Areas of the state outside the current combined fire protection responsibility areas of the California Department of Forestry and Fire Protection and contract counties (combined here and denoted CDF), the U.S. Department of Agriculture's Forest Service (USFS), and the U.S. Department of Interior's National Park Service (NPS), the Bureau of Land Management (BLM), and the Bureau of Indian Affairs (BIA) have been excluded.

A political boundary for California was extracted from the maps library in the statistical package R (http:www.r-project.org) and intersected with a 1/8-degree grid of polygons using the sp and gpclib libraries in R to create a grid with cell areas bounded by the State of California. This layer (CA.layer) served as the basis for deriving the rest of the data sets used in this analysis, and allowed us to calculate the area of each grid cell contained within the state.

Five time periods are used for this analysis. Statistical wildfire models are estimated using historical fire and climate data available for 1980–1999.[2] Model results from three future climate periods—2005–2034, 2035–2064, and 2070–2099 (henceforth referred to as *2020, 2050,* and *2085*) are compared to a common reference period (1961–1990, henceforth *1975*). Monthly aggregates for fire and hydroclimatic variables were compiled from daily data. The results presented here are annual averages for each 30-year period referenced above.

2.2. Fire History

A comprehensive wildfire history for California for 1980–1999 was assembled from digital fire records obtained from CDF, USFS, NPS, BLM, and BIA. The CDF records included perimeters for large fires under both direct CDF and contract counties' fire protection responsibility (obtained online at http://frap.cdf.ca.gov/). Federal fires were sourced from point data records compiled from individual fire reports. The methods used in compiling these data are described in Westerling et al. 2006 (online supplement) and Westerling and Bryant (2008). Westerling et al. (2002) describe in detail the federal data in this sample and their response to climate.

Our wildfire history was aggregated to a 1/8-degree gridded monthly data set of frequencies of fires > 200 ha in burned area and the total burned area in these large wildfires. Wherever we refer to *fire occurrence* in the text, we are referring to the occurrence of wildfires greater than 200 ha, unless otherwise specified. For federal-sourced wildfire data, fires were allocated to the grid cell in which they were reported to have ignited. For CDF fires reported as polygon perimeters, fires were allocated to the grid cell corresponding to their centroid using the maptools library in the R statistical package. Fires are assigned to the month in which they were discovered. In many cases fires continued to burn for additional months, but we did not have the means to apportion area burned by month.

Wildfires managed by the Fisheries and Wildlife Service (FWS), the Department of Defense (DOD), and the Bureau of Reclamation (BOR) were not were not included because they were not available with sufficient comprehensiveness and quality. The FWS and BOR lands are relatively small in area and—particularly in the case of FWS—located in areas (California's Central Valley) that would likely have been excluded from this analysis for other reasons. The Department of Defense lands in California are significant, similar in scale to those of NPS. We could extend our analysis spatially to DOD lands by applying model coefficients estimated using other agencies' fire histories to DOD lands, for which we have the explanatory variables. However, the vast majority of DOD lands in California lie in southeastern desert areas of the state, which show negligible changes in fire risks by the end of the twenty-first century under many, though not all, of our scenarios.

2.3. Land Surface Characteristics

2.3.1. Vegetation

Vegetation Characteristics

---

[2] Comprehensive fire data were available for 1980–2007, however the estimation period is limited to 1980–1999 because the suite of climatic and hydrologic data available for this study were simulated using observations ending in 1999.

Coarse vegetation characteristics used here were compiled from the Land Data Assimilation System (LDAS) for North America's 1/8-degree gridded vegetation layers that use the University of Maryland vegetation classification scheme with fractional vegetation adjustment (UMDvf) (Mitchell et al. 2004; Hansen et al. 2000). The UMDvf scheme has 14 coarse surface categories derived from 1 km AVHRR satellite data collected from April 1992 to March 1993. We combined these to obtain the four vegetation categories analyzed here: Forest (the Evergreen Needleleaf and Broadleaf Forest categories, the Deciduous Needleleaf and Broadleaf Forest categories, and the Mixed Cover category), Woodland (the Woodland and Wooded grasslands categories), Grassland (the Grassland category) and Shrubland (the Closed and Open Shrubland categories). We did not distinguish between evergreen and deciduous forest in this analysis because too little area of the latter was included in the study area to support a statistical analysis at a 12 km resolution. Note that vegetation characteristics are not used as predictors in any of the models presented here, but rather are used to analyze the modeling methodology.

Vegetation Fraction

We also consider another variable from LDAS—the fraction of each gridcell that is vegetated and not used for agriculture (V). In our model for estimating fire probabilities, V plays an important role. In the limit of complete urbanization, it is clear that this variable is affected by encroaching human development, because a gridcell entirely covered by dense population would lack any sufficiently large vegetated space in which wildfires could exist. However, vegetation cover may be reduced by encroaching human development at intermediate scales as well, depending on how new growth is allocated. In Section 2.4 and in more detail in the Appendix, we describe how scenarios for allocating projected growth within a gridcell affect the vegetation fraction. For the results reported here, the growth in urban areas reduces the vegetated areas proportionate to their current fraction of nonurban area (i.e., a portion of the urban growth consumes agricultural lands).

2.3.2. Topography

Topographic data on a 1/8-degree grid were also obtained from LDAS. The LDAS topographic layers are derived from the GTOPO30 Global 30 Arc Second (~1km) Elevation Data Set (Mitchell et al. 2004; Gesch and Larson 1996; Verdin and Greenlee 1996). We tested mean and standard deviation of elevation, slope, and aspect as explanatory variables in our wildfire model specification.

2.3.3. Protection Responsibility

Logistic regression techniques attempt to estimate probabilities of wildfires occurring at a given time and location as a function of predictor variables. The predictand is always valued zero or one, and in this case most data points are zero, since fires are relatively rare occurrences at ~12 km × monthly scales. It is important to distinguish between data points that are zero because no fire occurred, and data points that are zero because the fires that may have occurred there are not reported by the agencies included in our sample. The practical effect of including in our modeling areas for which we do not have good fire reports is to underestimate the probability of fire occurrence everywhere on average. We used the fraction of each grid cell's area covered by the protection responsibility of the agencies in our sample to estimate the area over which fires could occur.

A GIS layer of Local, State, and Federal protection responsibility areas in California was obtained online from the CDF Fire and Resource Assessment Program (http://frap.cdf.ca.gov/). Using the sp and gpclib libraries in R the polygons in this layer were extracted and intersected with the CA.layer described above to obtain the fraction of each grid cell in Local (LRA), State (SRA), and Federal (FRA) protection responsibility areas. Since federal protection responsibility includes agencies excluded from our sample, we obtained GIS layers of federal and Indian lands online from the United States National Atlas (http://nationalatlas.gov/). These were also extracted and intersected with CA.layer in order to determine what fraction of the federal responsibility area in each grid cell corresponded to the federal agencies in our sample.

Our analysis is limited to the SRA (for which we have CDF wildfire histories) and those parts of the FRA administered by the federal agencies for which we have wildfire histories (USFS, NPS, BLM, BIA). The LRA is excluded both because we do not have wildfire histories for those lands and because they are predominately developed for urban and agricultural uses. We limit our analysis to gridcells with a combined protection responsibility (SRA, USFS, NPS, BLM, BIA) exceeding 15% of the total gridcell area.

2.4. Growth and Development Scenarios

We employ a spatially explicit 100 m-resolution twenty-first century population growth and development scenario based on work by Theobald (2005) and developed by the U.S. EPA (2008) as one of the Integrated Climate and Land Use Scenarios (ICLUS) for the United States. These scenarios incorporate assumptions about future trajectories with regards to sprawl as well as population growth rates based on the Intergovernmental Panel on Climate Change (IPCC) *Special Report on Emissions Scenarios* (SRES) social, economic, and demographic storylines, downscaled to the United States. We report results here for a base case scenario with growth and sprawl intermediate between what would be consistent for the global A1 and B2 SRES scenarios, with statewide population increasing 84% over the year 2000 by 2100 to over 60 million (denoted as the MID growth scenario).[3] While we do not model spatial variation in wildfire below the 1/8-degree grid threshold, we do consider effects of assumptions about the allocation of new development below that level (described in detail in the Appendix). Our scenarios for allocating development consider the effects of expanding the wildland-urban interface into areas that are currently vegetated versus siting new development in areas that are currently bare or agricultural land. For the results presented here, we allocate new development proportionately across baseline vegetated, bare and agricultural areas (also denoted MID, so the combined growth and allocation scenario considered in this work at present is denoted the *MIDMID* scenario). Additionally, we use two different thresholds for describing when a 100 m pixel is fully "urbanized," such that a wildfire cannot occur there: 147 and 1000 households per square kilometer.

---

[3] Note that California growth scenarios do not have to match the global trajectory. For example, the state might successfully implement policies—or economic conditions might have similar effects—that restrict population growth and/or reduce its development footprint.

2.5. Climate and Hydrologic Data

2.5.1. Historical Data

A common set of gridded historical (1950–1999) climate data including maximum and minimum temperature, precipitation (PCP), radiation, and wind were designated for the California Scenarios 2008 project (see Maurer et al. 2002; Hamlet and Lettenmaier 2005). We used these data with LDAS vegetation and topography to drive the Variable Infiltration Capacity (VIC) hydrologic model at a daily time step in full energy mode, generating a full suite of gridded hydroloclimatic variables such as actual evapotranspiration (AET), soil moisture, relative humidity (RH), surface temperature (TMP) and snow-water equivalent (SWE) (Liang et al. 1994). Because Potential Evapotranspiration (PET) was not easily extracted from the version of the VIC model used here, we used the Penman-Monteith equation to estimate PET directly (Penman 1948; Monteith 1965). Moisture deficit (D) was then calculated from PET and AET (D = PET - AET). As in Westerling et al. (2006, online supplement), we adjusted D to equal zero on those days when there was some (>1 millimeter [mm] SWE) snow on the ground, to correct for the fact that the VIC model does not take account of sublimation in calculating AET. Without this adjustment, we would have small, erroneous moisture deficits on some days when there was some snow cover on the ground.

As indicators of drought stress, we calculated the cumulative water-year moisture deficit for each current year (D00), as well as for each of the preceding two years (D01 and D02). We also calculated the cumulative moisture deficit from October 1 through the current month (CD0), which was standardized by dividing by the 30-year (1961–1990) standard deviation (sD30) (e.g., CD0 is really CD0/sD30).

The 30-year means for 1961–1990 for moisture deficit (D30), AET (AET30), PCP (PCP30), and TMP (TMP30) were also used below to analyze the spatial distribution of climate-vegetation-wildfire interactions to be represented in the wildfire model specification (Section 3.1).

2.5.2. Climate Scenarios

As described by Cayan et al. (2008, this set of scenario reports), several GCMs and emissions scenarios were selected for the California Scenarios 2008 studies. In this report we describe results across three models—CNRM CM3, GFDL CM21, NCAR PCM—and two emissions scenarios—SRES A2 (a medium-high emissions trajectory) and SRES B1 (a low emissions trajectory) comprising six realizations for future climate. Daily climate data from these models were downscaled to the 1/8-degree grid using the Constructed Analogues method (see Hidalgo et al. 2008; Maurer and Hidalgo 2008). After downscaling, the VIC model was used to simulate the same suite of hydrologic variables for each target time period (2020, 2050, 2085) in each climate scenario as described for the historical period (Section 2.5).

As described in Cayan et al. (2008, this set of reports), the models were selected for their fidelity in representing historical California temperature and precipitation in particular, with appropriate seasonality. Also, the selected models were required to simulate tropical Pacific sea surface temperature variability consistent with observed ENSO variability, and to have appropriate spatial resolution over California for the downscaling methodologies employed here. That left a set of six models. Daily precipitation and daily maximum and minimum temperature had to be included in the models' historical and projection saved sets in order to

use the Constructed Analogs downscaling methodology, which narrowed the set to three models.

While we only use the three models downscaled with the Constructed Analogs methodology, the larger set of six models show a consensus toward drier conditions in southern and central California, but more scattered results in the region from Lake Shasta to the northernmost parts of California. An unpublished review of a larger set of 12 models showed similar results, increasing our confidence that the models used here are representative of what a larger set of models project for California.

So while it is true that our models do not encompass the full range of model uncertainty of the AR4, limited resources necessarily constrain the scope of the study. That said, these models appear to cover a range of projected temperature and precipitation that is representative of the state of the art modeling guidance for California.

Each of the GCMs evidences different sensitivities to anthropogenic forcing, with the CNRM CM3 and GFDL CM21 models generally showing warmer temperatures than the NCAR PCM, particularly in summer. The GFDL CM21 model tended to be drier than the others in both northern and southern California in most scenarios, while CNRM CM3 was typically drier than NCAR PCM. It is not clear to what extent the variation in precipitation across the models is due to random factors, since two realizations of each of three models is a small number compared to the potential natural variability in precipitation in the region. Notably, the tendency towards dryness across all the models is much more pronounced and uniform for California in the A2 emissions scenarios, when anthropogenic forcing is higher, than for the B1 scenarios, and it seems reasonable to speculate that the forcing is overwhelming the natural variation in the A2 scenarios.

The six climate scenarios used here encompass three separate sources of uncertainty for our modeling: the degree of anthropogenic forcing (represented by the A2 and B1 emissions paths), the extent of climate system sensitivity to anthropogenic forcing (greater in GFDL CM21 and CNRM CM3 than NCAR PCM), and the range of random variation in climate across 30-year windows in six scenarios (unknowable for a sample of this size).

3.0 Modeling

3.1.   Fire-Climate-Vegetation Interactions

When modeling large wildfire occurrence statistically for seasonal forecasts, Preisler and Westerling (2007) include smoothed location-specific terms that implicitly estimate the combined effect of idiosyncratic factors on wildfire risks, such as the availability of ignitions, characteristics of local vegetation, topography, accessibility, and suppression resources. Using fixed parameters like these is appropriate for forecasting a season or a month in advance, since these effects tend not to change dramatically on such short time scales. In modeling for scenario analyses one hundred years hence with very different climates, human populations and development footprints, however, it is necessary to incorporate explicit terms for those effects that will likely change, so that they can vary appropriately with the scenarios considered.

By incorporating variables such as population and vegetation fraction directly into our model, we can capture some of these effects directly. However, we must also consider how the spatial

distribution of vegetation types might change over time. As the spatial distribution of vegetation types changes, the spatial patterns in fire regime response to climate variability will also shift. To ensure selection of a model specification that captures the spatial pattern of vegetation and fire regime response to climate, we analyze the links between long-term average climate and both vegetation and wildfire.

We do not incorporate vegetation characteristics directly into our fire models as predictors—instead we use long-term average climate parameters as proxies for both vegetation and fire regime type. However, in this section we associate those parameters with coarse vegetation types to analyze the implications of the model specifications described in Section 3.2 below.

Stephenson (1998) tested the power of various climate indices to describe the spatial distribution of coarse vegetation types and concluded that a combination of average cumulative annual AET and D performed best. We considered both AET30 × D30 (Figure 1) and PCP30 × TMP30 (not shown, see Westerling 2008, in press). Both approaches performed similarly in their ability to distinguish between the four vegetation types used here for descriptive purposes (Forest, Woodland, Grassland, and Shrubland), while AET × D was a superior predictor for spatial variation in large wildfire occurrence in California. In Figure 1 (top left) we show vegetation characteristics plotted against quintiles of average AET30 and D30. The colors in the pie charts show the distribution of vegetation characteristics across all the grid cells binned within each climatic quintile, while the area of each pie chart is scaled to show the relative area in those grid cells as a fraction of the total protection responsibility in our spatial domain.

Note the concentration of forested area in gridcells with high AET30 and low D30 (dark green areas, upper left corner of Figure 1, top left panel): these are relatively moist areas where AET is not severely limited by available moisture, and where the average deficit is consequently low. Note also that our sample is skewed toward a large percentage of Forest and Woodland vegetation types (dark green and light green pie sections, respectively, in Figure 1, top left panel) because these are types that have been preferentially preserved on public lands and rural private holdings that have not been converted to agriculture and urban uses. It is also true that the DOD lands excluded from our analysis comprise a substantial fraction of the drier locations within the state.

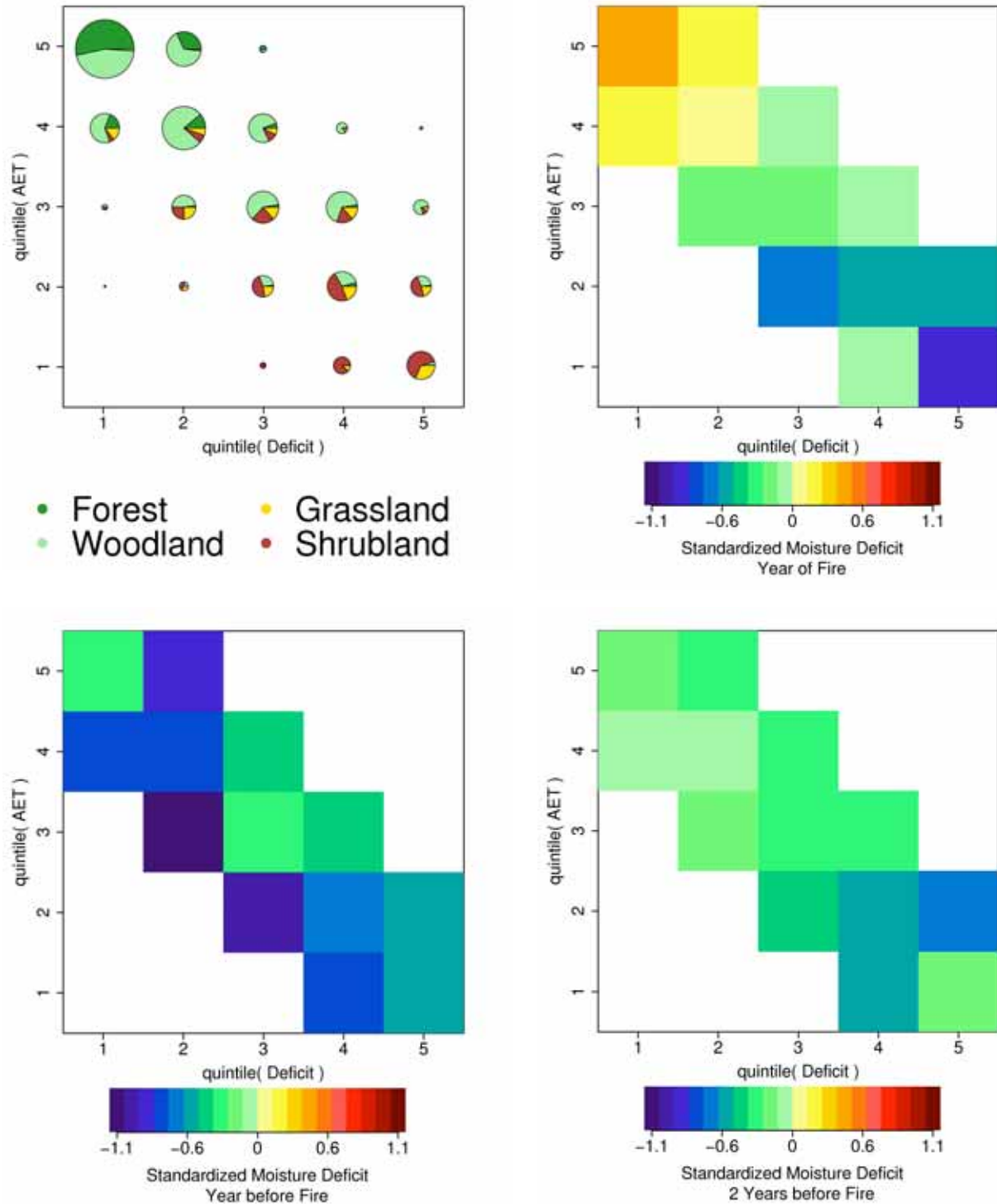**Figure 1. Vegetation versus 1961–1990 mean Oct.–Sep. cumulative Deficit and AET (top left), with area scaled to fraction of protection responsibility. Standardized Deficit composited for fires > 200 ha, for year of fire (top right), year prior to fire (bottom left), and two years prior (bottom right). Warmer colors indicate drier than average conditions, and cooler colors indicate wetter than average conditions.**

The quintile with a high concentration of forested area also exhibits a distinct pattern of climate-wildfire interactions, with dry conditions the year of the fire and neutral conditions in preceding years (Figure 1). This is indicative of an energy-limited wildfire regime, where fuels are typically sufficient to carry a large wildfire, but fuel flammability is a limiting factor for the ignition and rapid spread of wildfires.

Conversely, areas with drier conditions (lower AET30 and higher D30) tend to have higher proportions of grass and shrublands, and fires tend to occur after one or more wet seasons (Figure 1). These patterns are indicative of wildfire regimes where flammability is typically less of a limiting factor on large fire occurrence, and where the availability of fuels is more important (see Westerling et al. 2002; Westerling 2008, in press).

These relationships demonstrate that an interaction between AET30 and D30 can serve as a proxy for fire regime type and coarse vegetation characteristics. By interacting variables that capture monthly to interannual variation in climate with variables that describe the AET30 × D30 interaction, we can capture spatial variation in fire regime response to climate variability. By using long-term average AET and D for future time periods and scenarios (e.g., estimating AET30 and D30 with values from 2005–2034 for the SRES A2 emissions scenario and the CNRM CM3 model), we can model spatial shifts in vegetation and fire regime. The essential assumption inherent in this approach is that the current coarse-scale climate, vegetation and fire patterns observed in the region provide examples that encompass future regimes. To the extent that entirely novel situations might arise in the future, this assumption may provide misleading results. However, this is the same assumption that underlies the Constructed Analogues downscaling method, and in that approach very few days arise in climate scenarios that do not have contemporary analogues.

3.2. Fire Modeling

Because large wildfires are relatively rare events, statistical models for wildfire must aggregate fire occurrence over space and/or time in order to avoid fitting a model of zeros. Logistic regressions allow us to model wildfire occurrence at arbitrarily fine spatial and temporal resolutions (limited only by the available data) while statistically aggregating across locations with similar characteristics. We estimate the probability of large (> 200 ha and > 8500 ha) wildfires occurring as a function of land-surface characteristics, human population, and climate.

The climatic variables used here as predictors for fire occurrence (Table 1) were selected to describe variation in moisture available for the growth and wetting of fuels over a range of time scales, from long term averages over thirty years (D30, AET30), to interannual variations in the three years through the current year (D01, D02), to seasonal variations and conditions at the month a fire could potentially burn (CD0, RH, TMP). Westerling and Bryant (2008) and Westerling (2008 in press) show that long-term climate averages can serve as a proxy for coarse vegetation and fire regime types, distinguishing between diverse fire regime responses to antecedent and concurrent climate. Westerling (2008 in press) and Westerling et al. (2006) show that cumulative annual moisture deficits in the current and 1–2 preceding years are strongly associated with variability in large wildfire occurrence, and the latter work also links large wildfire occurrence to temperature and variations in spring snowmelt timing. Finally, relative humidity (RH) is a key component of many fire weather indices, and a good predictor of fuel moisture (e.g., Schlobohm and Brain 2002).

Table 1. Predictor variables

Variable	Description	> 200 ha[1]	> 8500 ha[2]
D30	30-year average cumulative Oct.–Sep. moisture deficit	√	√
AET30	30-year average cumulative Oct.–Sep. actual evapotranspiration	√	√
D02	Cumulative 0ct.–Sep. moisture deficit, two years previous	√	
D01	Cumulative 0ct.–Sep. moisture deficit, one year previous	√	
CD0	Cumulative moisture deficit, Oct. through current month	√	
RH	Monthly average Relative Humidity	√	√
TMP	Monthly average surface air Temperature	√	√
V[3]	Vegetation Fraction	√	
POP	Total population (2000)	√	
FRA[3]	Federal protection responsibility area as percent of total area	√	
USFS[3]	USFS protection responsibility area as percent of total area		√
Aspect[4]	Average north/south facing		√

[1] Predictors for logistic regression estimating probability of a fire exceeding 200 ha.

[2] Predictors for logistic regression estimating probability total burned area exceeds 8500 ha conditional on one fire having exceeded 200 ha.

[3] Fractions are transformed using log((fraction+.002)/(1-fraction+.002)) to generate a continuous variable centered around zero.

[4] The transformation cos(pi/2+aspect*pi/180) yields the north/south component of aspect.

Vegetation fraction and population are indicators of burnable area, availability of human-origin ignitions, and accessibility. Other variables we tested—such as total protection responsibility area, and mean and standard deviation of elevation—were not included in the model specification because they either did not improve model fit as measured by the Akaike Information Criterion generated by the glm() function in R, or their addition introduced singularities that prevented estimation of a model. The climatic and land surface variables we selected are not independent of topography and protection responsibility area. Federal protection responsibility and U.S. Forest Service protection responsibility area were highly significant, and may be indicative of differences in management or resources across protected areas, or they may be proxies for other spatial variables such as accessibility, vegetation type, sources of ignitions, etc.

The model specification employed here for estimating fire occurrence builds on Preisler and Westerling (2007) and Westerling and Bryant (2008), and adopts methodologies presented in Brillinger et al. (2003), and Preisler et al. (2004):

$$\text{Logit}(\pi_{200}) = \beta \times [\,1 + D30 + D01 + D02$$

$$+ X(D30,AET30) \times (\,1 + P(TMP) + CD0) + P(TMP) + P(RH)$$

$$+ P(POP) \times (\,1 + D30\,) + X(V) + FRA\,]$$

where π_{200} is the probability of a fire > 200 ha occurring, $\text{Logit}(\pi_{200})$ is the logarithm of the odds ratio $(\pi_{200}/(1-\pi_{200}))$, β is a vector of parameters estimated from the data, and X(•) and P(•) are matrices describing basis spline and polynomial transformations of the data. The interaction terms:

11

$$X(D30,AET30) \times (1 + P(TMP) + CD0)$$

result in estimation of a set of constants and a set of coefficients on average monthly temperatures and cumulative moisture deficits that are associated with the distribution of vegetation types and patterns of fire regime response to climate variability.

The interaction terms:

$$P(POP) \times (1 + D30)$$

capture direct effects of local population on the probability of large fire occurrence, which vary in this specification with the average summer moisture deficit in any given location. These factors may be indicative of several effects, including ignitions, accessibility, suppression resources, and suppression strategies.

We also estimate the probability that one or more very large fires burning in excess of 8500 ha in aggregate may occur, conditional on there being at least one fire exceeding 200 ha:

$$\text{Logit}(\pi_{8500|200}) = \beta \times [1 + X(D30,AET30) \times TMP + RH + Aspect + USFS]$$

This model says that whether or not a large fire becomes a very large fire or not depends on the temperature interacted with fire regime type, the relative humidity, the north/south facing, and whether the fire is on Forest Service land or not. The latter variable might be related to management strategies, or it could simply be that so much of the forested area of the state, especially in less accessible locations, is managed by the Forest Service.

We estimate generalized Pareto distributions (GPDs) for the logarithm of burned area for fires > 200 ha and for fires > 8500 ha (for a discussion of methodology as it applies to wildfire and evidence that fire size regimes are consistent with heavy-tailed Pareto distributions, see Straus et al. 1989; Malamud et al. 1998; Ricotta et al. 1999; Cumming 2001; Song et al. 2001; Zhang et al. 2003; Schoenberg et al. 2003; Holmes et al. 2008). From these we estimate the expected area burned for a fire given that its area is greater than 200 ha and less than 8500 ha, and the expected area burned for fires given that they are > 8500 ha. We use a two-step process like this because the empirical distribution of fire sizes in California appears to be non-stationary. Extremely large fires are governed by different processes than are more frequent large fires.

3.3.   Migration of Fire Regimes and Ecosystems

As climatic conditions shift farther and farther from what pertained in the reference period, the spatial distribution of vegetation types, and therefore of fire-climate relationships, is likely to shift. When and how that occurs is a major source of uncertainty in modeling wildfire under climate change scenarios. Rather than gradually adjusting in step with changes in climate, spatial patterns in vegetation may persist until some disturbance such as fire, drought, or insects triggers an abrupt reorganization. In cases where climate change is likely to result in a substantial shift in vegetation types in a given location, the fire regime response to climate variability there will be bounded by, on the one hand, behavior expected of the original vegetation and, on the other hand, by behavior expected of some new assemblage of vegetation, interacting with the climate system.

It would be a mistake to make an impact assessment an exercise in comparative statics, because such an analysis would be likely to miss the potential for large disturbances during transition periods. While we cannot easily anticipate the timing of disturbance-driven transitions, we can vary our model specification to try to bound changes in fire occurrence.

In this treatment, for future scenario periods we approximate fixed fire regimes ("non-migration") by holding D30 and AET30 fixed at their 1961–1990 values, and similarly the scaling factors used to standardize cumulative moisture deficit (see Section 2.5.1) are also held fixed. To simulate migration, we recalculate these values using downscaled and simulated hydroclimatic variables for each future 30-year period analyzed.

3.4. Summary of Scenarios

To summarize, we estimate 72 future scenarios, varying our model specification for *migratation* versus *no migratation* over two emissions scenarios, three GCMs, two thresholds for defining urbanization, three scenarios for growth rates and the allocation of development, and three future time periods (Table 2).

Table 2. Summary of scenarios

Adaptation	Emissions	Model	Urban Threshold (households/km^2)	Growth Rate & Allocation	Period
True	SRES A2	CNRM CM3	147		2020
False	SRES B1	GFDL CM21	1000	MID, MID	2050
		NCAR PCM1			2085

4.0   Results and Discussion

4.1.   Model Fit

The statistical significance of coefficients for the wildfire model specification was very stable across sub-samples, using jackknife cross-validation. The logistic regression for fires greater than 200 ha fit the observations well (Figure 2), and the maximum probability of predicted fire occurrence was over 23%, which compares well with earlier fire models for climate change impact assessments in Westerling and Bryant (2008) and seasonal forecasting in Preisler and Westerling (2007). The scale of interannual variation in expected fires aggregated statewide was comparable to that of observed fire. Forty percent of interannual variability in statewide large (> 200 ha) wildfire occurrence was explained by the predicted probabilities, and the correlation between annual observed fire occurrence and predicted fire occurrence was highly significant (Spearman's ρ = 0.74, p-value = 0.0002). For monthly fire occurrence aggregated statewide, 58% of month-to-month variability was explained, and the correlation was also highly significant (Spearman's ρ = 0.84, p-value = 2e-16). The additional skill at the monthly time scale is due to the model fitting the seasonal cycle in the incidence of fires > 200 ha, as well as the interannual variability.

Results for our estimation of the frequency of fires greater than 8500 ha were also significant, but the skill was lower. This is likely due to both the small number of observed fires of this magnitude, and also it is likely that the size of these fires is highly sensitive to factors we are not able to consider here, such as the management strategy on individual fires, meteorological

conditions on hourly to daily timescales during the fire, and landsurface characteristics at finer scales than those practical here (~12 km). Nineteen percent of interannual variability in statewide very large (> 8500 ha) wildfire occurrence was explained by the predicted probabilities, and the correlation between annual observed and predicted very large fire occurrence was significant (Spearman's ρ = 0.44, p-value = 0.05). Similarly, monthly predicted very large fire occurrence explained 25% of the variation in observed monthly values, and the correlation was highly significant (Spearman's ρ = 0.46, p-value < 2e-16).

While the Generalized Pareto Distribution fit the logarithm of monthly burned areas exceeding 200 ha and 8500 ha very well (Figure 3), the empirical fire size distributions still have a "fatter" right tail (i.e., higher probability of extremely large fires) than estimated by the modeled distributions, as indicated by the values to the far right in the Quantile plots sitting above the 1:1 ratio line (Figure 3). This means that the resulting expected burned area estimates tended to underestimate the average area burned. For the model estimation period, average area burned was underestimated by just under 19%. Burned area in a small number (< 10) of months over the 20-year estimation period far exceeded our predictions and accounts for the underestimated area (Figure 4). The correlation between predicted and observed burned area was highly significant (Spearman's ρ = 0.81, p-value < 2e-16).

Generalized Pareto Distributions can be fit with covariates such as climate and landsurface characteristics, such that the parameters describing the distribution vary over time and space (see e.g., Holmes et al. 2008). We tested the full suite of predictor variables described in the preceding sections. While some of them were highly significant statistically, in practice including covariates had a trivial impact on our ability to predict year-to-year variations in burned area. Consequently, the results reported here use GPD fits assuming stationarity (i.e., that the fire size distribution does not change over time). Thus, the interannual variation in our predicted burned area is due entirely to variation in estimated probabilities for burned area to exceed the two specified thresholds (200 ha and 8500 ha).
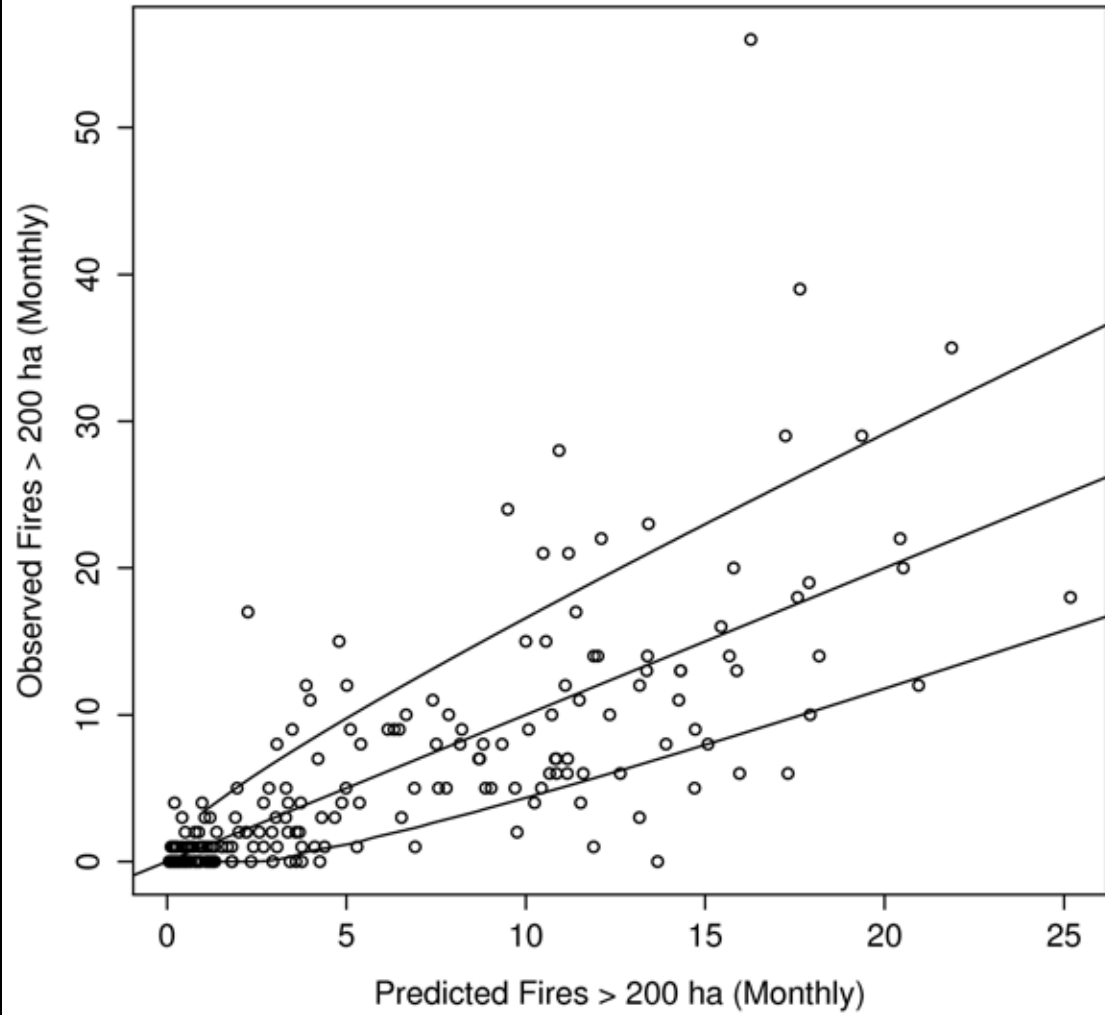
Figure 2. Logistic regression model fit for fires > 200 ha: Observed fire frequency (vertical axis) versus predicted probabilities (horizontal axis), binomial 95% confidence interval (upper and lower lines).

GPD Fit: Burned Area > 200 ha   GPD Fit, Burned Area > 8500 ha
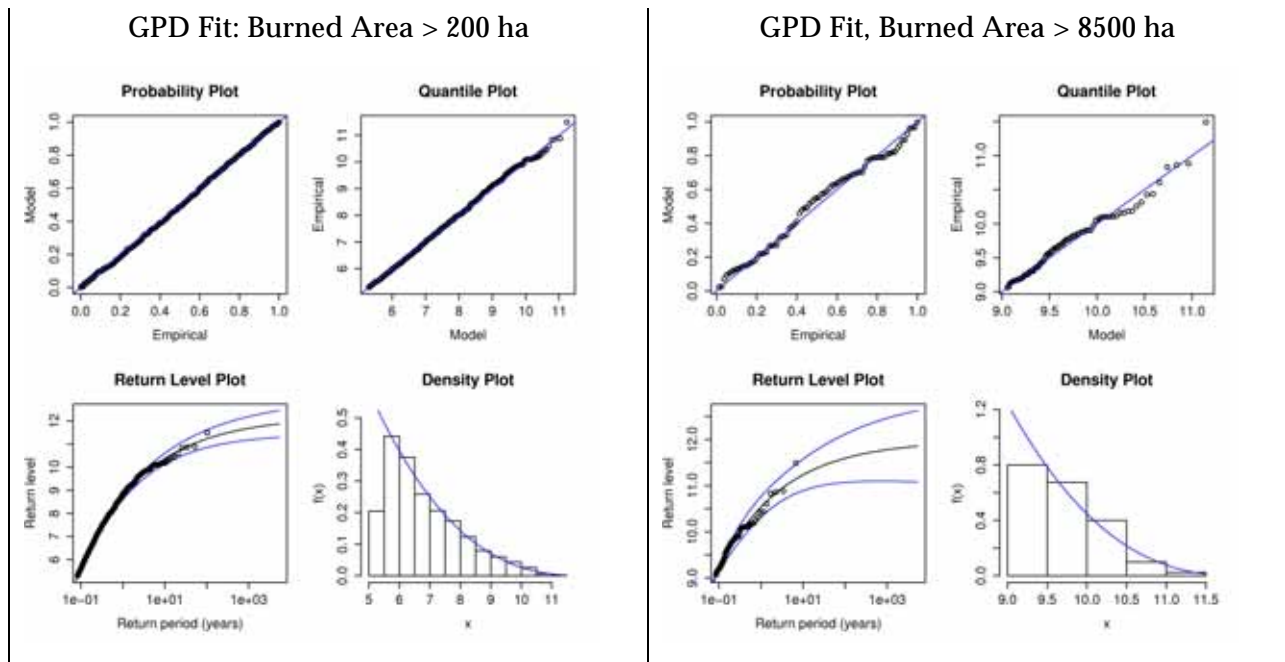
Figure 3. Generalized Pareto Distributions fit to occurrence of burned area > 200 ha (left) and burned area > 8500 ha (right). Distributions are fit to the logarithm of burned area and assume stationarity.

California Monthly Burned Area

(vertical axis: observed burned area (hectares); horizontal axis: predicted burned area (hectares))
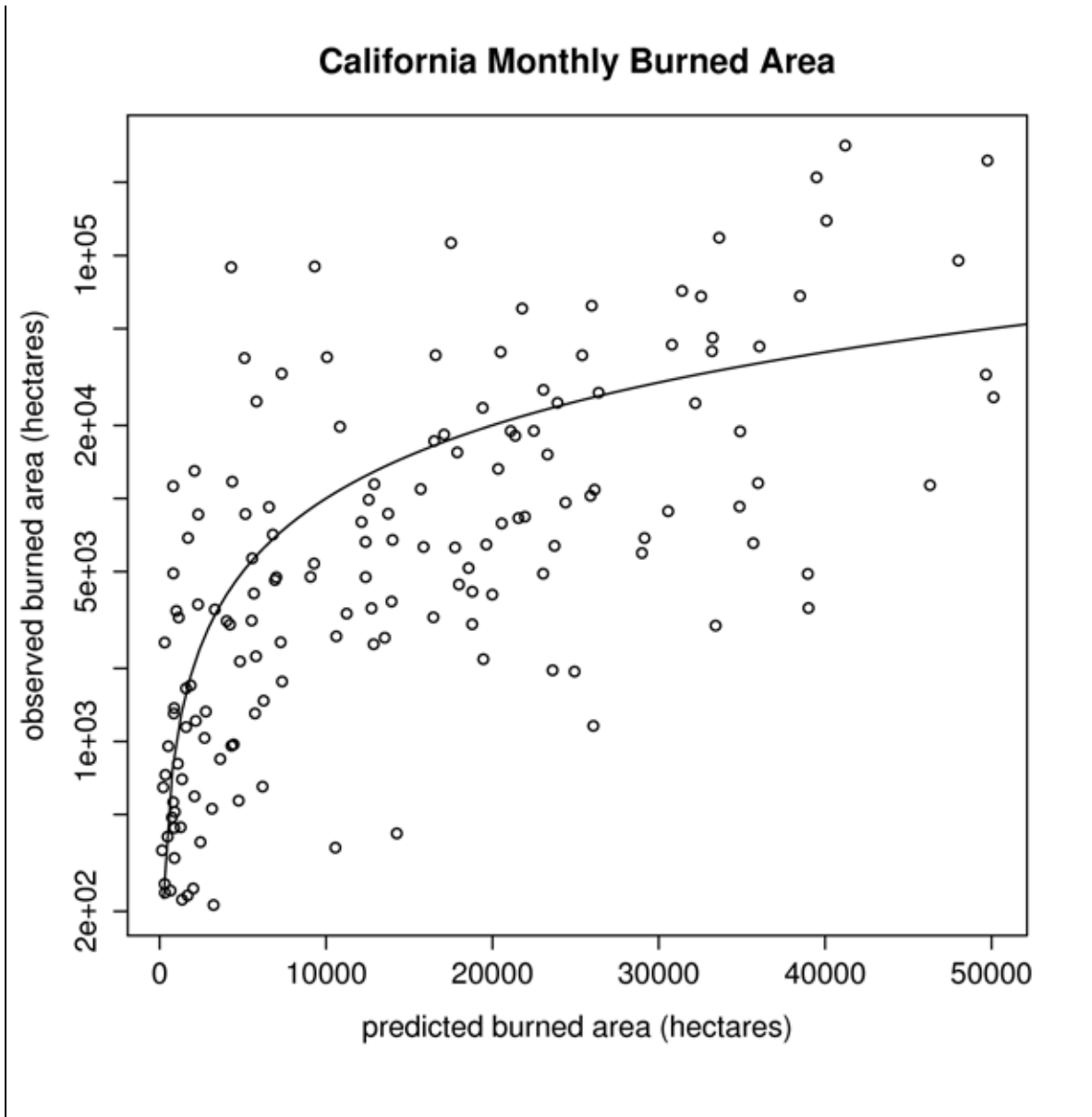
Figure 4. Predicted (horizontal axis) versus observed (vertical axis) burned area for large fires in California. The vertical axis is on a logarithmic scale. The curved line represents the 1:1 ratio between predicted and observed burned area.

4.2. Changes in California Wildfire

Predicted large fire occurrence and total area burned increase across all scenarios (Tables 3 and 4, Figure 5). Initial increases for both parameters are relatively modest—by 2020 the minimum increases cluster around 10%, median increases cluster around 20%, and the upper bound ranges from 30% to 41% increases (Tables 3 and 4). By 2050 the spread in modeled outcomes widens, with predicted increases in large fire occurrence ranging from 11% to 55%, and median increases around 30%. Similarly, by 2050, burned area is predicted to increase anywhere from

11% to 70%, again with median increases around 30%. By 2085, the range of modeled outcomes is very large (Tables 3 and 4, Figure 5), with large fire occurrence increasing anywhere from 25% to 128% and burned area increasing 23% to 169%. It is notable that, while the range of outcomes is very broad, the minimum increase in area burned is 25% (for SRES B1 NCAR PCM1). The largest increases occur in 2085 for SRES A2 scenarios, with the minimum increase in fire occurrence (58%, Table 3) exceeding the highest predicted increases (53%) previously estimated for 2085 for the 2006 climate change impacts assessment (Westerling and Bryant 2008). Predicted increases in burned area for SRES A2 in 2085 are very large, ranging from 57% to 169%

Table 3. Summary statistics for statewide predicted large (> 200 ha) wildfire occurrence, expressed as percent of the 1961–1990 reference period

	2005–2034			2035–2064			2070–2099		
SRES	Min	Median	Max	Min	Median	Max	Min	Median	Max
A2	108	121	132	118	133	155	158	184	228
B1	112	117	130	111	128	145	125	138	165

Table 4. Summary statistics for statewide predicted burned area, expressed as percent of the 1961–1990 reference period

	2005–2034			2035–2064			2070–2099		
SRES	Min	Median	Max	Min	Median	Max	Min	Median	Max
A2	107	122	141	117	137	170	157	207	269
B1	112	121	138	111	127	158	123	143	180

The SRES A2 scenarios in 2085 seem to be qualitatively different from either earlier periods or SRES B1 in 2085 (Tables 3 and 4, Figure 5), implying that the most important policy implication of this study may be that moving to an emissions pathway more like that in SRES B1 (or lower) could be highly advantageous.
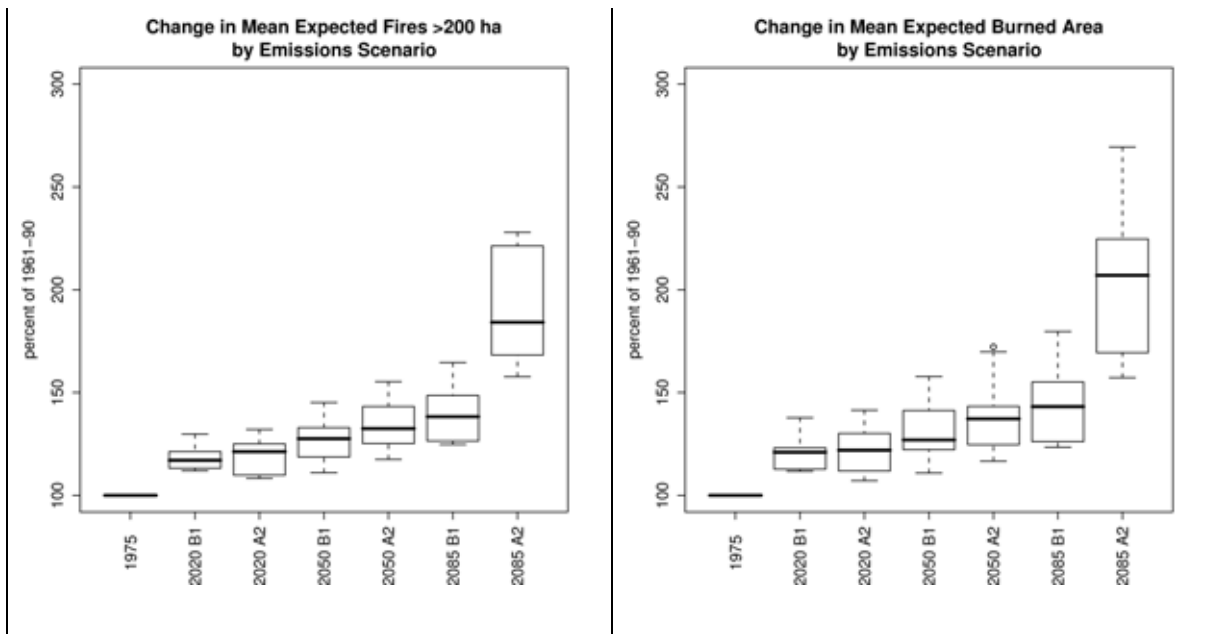
Figure 5. Expected fires for California as a percentage of 1961–1990 reference period for 96 scenarios, estimated for 30-year periods centered on the indicated dates, by emissions scenario. Bold horizontal lines indicate median scenario, boxes indicate middle 50% of values, whiskers indicate extremes.

Allowing wildfire regimes and vegetation characteristics to migrate in response to climate change tended to increase both the range and the median for predicted burned area (Figure 6) and fire occurrence (not shown). However, the dramatic increases in SRES A2 in 2085 as compared to SRES B1 or earlier periods for either model (Figure 5) are not merely artifacts of the migration/no-migration model specifications, since the results for 2085 show large shifts relative to earlier periods regardless of the migration/no-migration specification (Figure 6).

Some of the greatest differences between the two specifications are in the spatial patterns of fire occurrence and burned area. In a set of GFDL CM21 and CNRM CM3 scenarios for SRES A2 in 2085, for example (Figure 7), migration of fire regimes produces greater increases in wildfire burned area across much of the state, but in particular burned area increases in coastal southern California and the Monterey Bay area. Across all four scenarios, burned area increases exceed 100% or more throughout most of the forested areas of Northern California (and equal or exceed 300% for much of that area in the SRES A2 GFDL CM21 scenarios). The SRES A2 NCAR PCM1 scenarios (Figure 8) follow the same spatial patterns as the scenarios in Figure 7, with statewide average increases corresponding to the lower end of the ranges in Table 4 (i.e., > 50%) and increases on the order of 100% in large portions of Northern California forests. A robust result of this study is that forest burned area increases substantially—exceeding increases of 100% throughout much of the forested areas of Northern California—across all three of the GCMs analyzed here for the SRES A2 emissions scenario by 2085, under both fire model specifications.
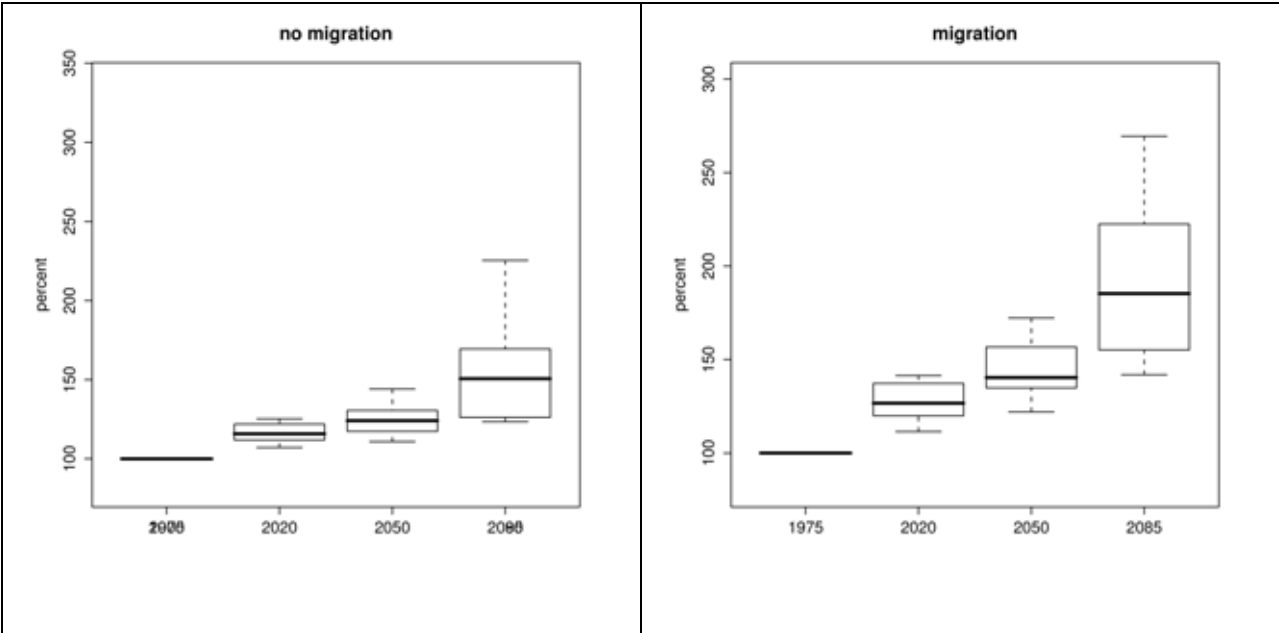
Figure 6. Change in expected burned area using model specifications with and without migration of vegetation and fire regime types, expressed as percent of reference period predicted average statewide burned area
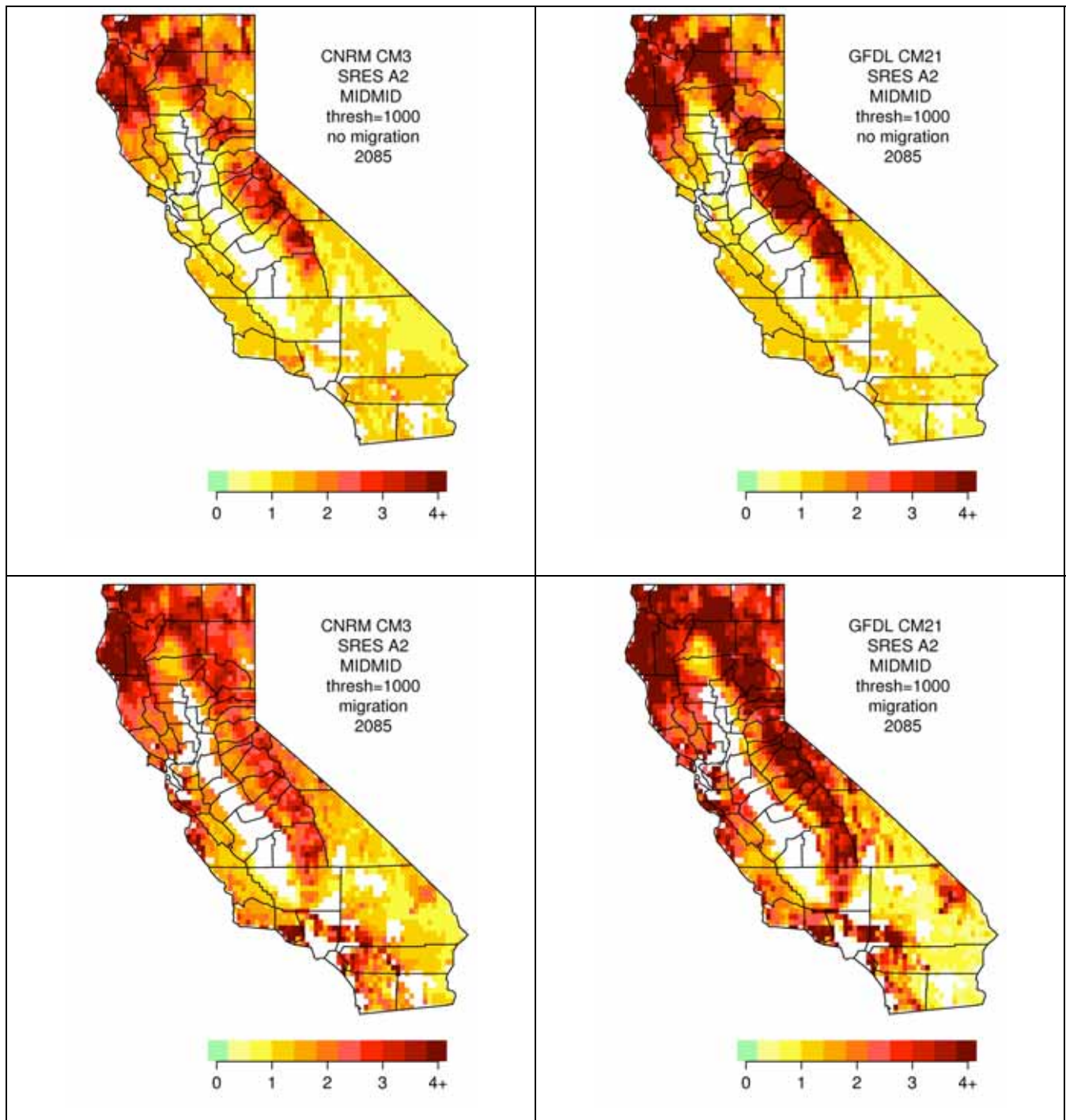
Figure 7. 2085 Predicted burned area as a multiple of reference period predicted area burned. Top panels show SRES A2 scenarios with the location of fire regimes fixed, while bottom panels simulate fire regimes (and ecosystems) shifting in response to changes in climate. All four scenarios show large increases in burned area in forests of the Sierra Nevada, northern California Coast, and southern Cascade ranges. With migration of fire regime types, burned area increases in coastal southern California and the Monterey Bay area. A value of "1" indicates burned area is unchanged, while 4+ indicates that burned area is 400% or more of the reference period.
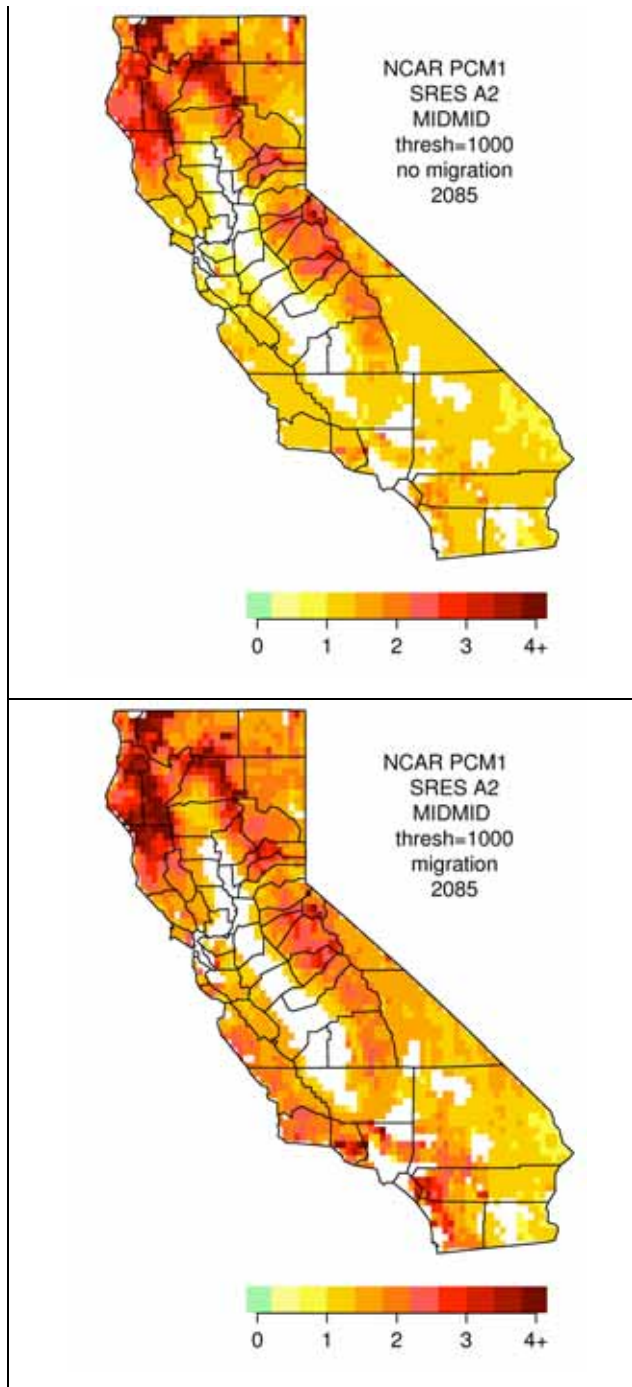
Figure 8. Predicted burned area in 2085 as a multiple of reference period predicted area burned for SRES A2 NCAR PCM1 scenarios with (top) the spatial location of fire regimes and ecosystem types fixed and (bottom) fire regimes and ecosystems shifting in response to changes in longterm climatic. Like SRES A2 GFDL CM21 and CNRM CM3 scenarios (Figure 7), these show large increases in burned area in forests of the Sierra Nevada, northern California Coast, and

5.0   Conclusion

We examined a range of future scenarios, considering multiple GCMs, emissions scenarios, and model specifications, and employing one growth and development scenario that falls between what would be consistent for the global SRES A2 and B1 storylines. While the range of outcomes for these scenarios was large by mid and late century, a majority of the scenarios indicated significant increases in large wildfire occurrence and burned area are likely to occur by mid-century under the model specifications and assumptions employed here. By 2085, very large increases in large wildfire occurrence and burned area seem likely, particularly under the SRES A2 emissions scenarios. The latter is mainly due to the effects of projected temperature increases on evapotranspiration in this scenario, compounded by reduced precipitation. The middle 50% of scenarios for 2085 ranged from average statewide burned area increases of 69% to 125% compared to the reference period centered around 1975 (Figure 5).

The spatial pattern of increased fire occurrence and burned area appeared to depend in part on the timing of changes in vegetation (Figures 7 and 8). However, it is important to note that wildfire burned area increased dramatically throughout the mountain forest areas of Northern California across all of the various 2085 SRES A2 scenarios examined here. The SRES A2 scenarios by 2085 were qualitatively different from the B1 scenarios and the earlier period A2 scenarios in terms of (the scale and spatial extent of increased fire occurrence and burned area). Given that we do, as a species, face choices regarding future emissions pathways, it would seem desirable to avoid persisting on a high greenhouse gas emissions pathway like A2

As noted in a companion study (Bryant and Westerling 2009, this set of reports), the results presented here reflect a set of illustrative models and their underlying assumptions that together result in a cascading series of cumulative uncertainties, such that results for any one time and location cannot be considered a reliable prediction, even contingent on the scenario represented. While Bryant and Westerling point out that aggregating results over time and space and comparing outcomes against a common reference period estimated with the same methods and data sets can reduce the impact of some types of systematic error, these measures are not foolproof. Nonlinear effects of errors, or qualitative systematic changes over time that are not captured by our models, can lead to significant errors in future projections that are not encompassed by the range of uncertainty represented in our results. That is, the results are conditional not only on the storylines of the SRES A2 and B1 scenarios and choice of global climate models, but also on the specifications of the statistical models of fire activity that we have estimated from historic data. To the extent that these data reflect processes that will no longer operate in the future because of qualitative changes to the systems we are modeling, our results will be in error.

Our results project the current managed fire regimes of California onto future scenarios for climate and for population and development footprint. We do not consider hypothetical effects of future changes in management strategies, technology, or resources that might be adopted with the intent of mitigating or adapting to the effects of climate and development on wildfire. Our models' implicit assumptions that such management effects are fixed may prove untenable

under some future scenarios. Explicitly including management factors that can vary over the long term might significantly affect the outcomes modeled here in a systematic fashion. Such an exercise is left to a future study.

While we do not model metrics of fire severity (e.g., percent of vegetation consumed, ecological impact of burning) here, we expect that fire severity will be correlated with increases in fire occurrence and spatial extent in some ecosystems, particularly in the mountain forest areas of the state. It is possible that increased fire occurrence and burned area in coastal southern California could coincide with decreased severity as assessed by some metrics if occasioned by a shift from chaparral- to grass-dominated fire regimes (excluding the possible effects of invasive species). While reduced severity there might ameliorate impacts on property losses, the ecological implications would still make this an undesirable outcome. It seems likely that outcomes such as those described here would have important implications for ecosystem services such as carbon sequestration in California forests, air pollution and public health, forest products and recreation industries, and the quality and timing of runoff from precipitation and snowmelt. All of these merit intensive further study.

These results will be extended in the near future to incorporate growth and development scenarios for California that project higher and lower population growth trajectories and greater and lesser development footprints. This modeling approach could be easily applied to runs from additional GCMs as hydrologic simulations forced with climate data downscaled from those models are completed.

6.0   References

Balling R. C., G. A. Meyer, and S. G. Wells. 1992. "Relation of Surface Climate and Burned Area in Yellowstone National Park." *Agricultural and Forest Meteorology* 60:285–293.

Brillinger, D. R. , H. K. Preisler, and J. W. Benoit. 2003. "Risk assessment: a forest fire example." In Science and Statistics, Institute of Mathematical Statistics Lecture Notes. Monograph Series.

Cayan, D., M. Tyree, et al. 2009. Climate Change Scenarios and Sea Level Rise Estimates for the California 2008 Climate Change Scenarios Assessment California Climate Change Center. In preparation.

Cumming, S. G. 2001. "A parametric model of the fire-size distribution." C*anadian Journal of Forest Research* 31: 1297–1303.

Gesch, D. B., and K. S. Larson. 1996. Techniques for development of global 1-kilometer digital elevation models. In *Pecora Thirteen, Human Interactions with the Environment - Perspectives from Space.* Sioux Falls, South Dakota, August 20–22, 1996.

Hamlet A. F., and D. P. Lettenmaier. 2005. "Production of temporally consistent gridded precipitation and temperature fields for the continental U.S." *J. of Hydrometeorology* 6(3): 330–336.

Hansen, M. C., R. S. DeFries, J. R. G. Townshend, and R. Sohlberg. 2000. "Global land cover classification at 1km spatial resolution using a classification tree approach." *International Journal of Remote Sensing* 21:1331–1364.

Heyerdahl, E. K., L. B. Brubaker, and J. K. Agee. 2001. "Factors controlling spatial variation in historical fire regimes: A multiscale example from the interior West, USA." *Ecology* 82(3): 660–678.

Hidalgo, H. G., M. D. Dettinger, and D. R. Cayan. 2008. *Downscaling with Constructed Analogues: Daily Precipitation and Temperature Fields over the United States.* CEC Report CEC-500-2007-123. January 2008.

Holmes, T. P., R. J. Hugget, and A. L. Westerling. 2008. Statistical Analysis of Large Wildfires. Chapter 4 of *Economics of Forest Disturbance: Wildfires, Storms, and Pests,* Series: Forestry Sciences, Vol. 79. T. P. Holmes, J. P. Prestemon, and K. L. Abt, Eds. XIV, 422 p. Springer. ISBN: 978-1-4020-4369-7.

Kipfmueller, K. F., and T. W. Swetnam. 2000. Fire-Climate Interactions in the Selway-Bitterroot Wilderness Area. USDA Forest Service Proceedings RMRS-P-15-vol-5.

Liang, X., D. P. Lettenmaier, E. F. Wood, and S. J. Burges. "A simple hydrologically based model of land surface water and energy fluxes for general circulation models." *J. Geophys. Res.* 99(D7), 14,415–14,428. July 1994.

Maurer, E. P., A. W. Wood, J. C. Adam, D. P. Lettenmaier, and B. Nijssen. 2002. "A long-term hydrologically-based data set of land surface fluxes and states for the conterminous United States." *J. Climate* 15:3237–3251.

Malamud, B. D., G. Morein, D. L. Turcotte. 1998. "Forest fires: An example of self-organized critical behavior." *Science* 281:1840–1842.

Mitchell, K. E. et al. 2004. "The multi-institution North American Land Data Assimilation System (NLDAS): Utilizing multiple GCIP products and partners in a continental distributed hydrological modeling system." *J. Geophys. Res.* 109, D07S90, doi:10.1029/2003JD003823.

Monteith, J. L. 1965. "Evaporation and the environment." *Symp. Soc. Expl. Biol.* 19: 205–234.

Penman, H. L. 1948. "Natural evaporation from open-water, bare soil, and grass." *Proceedings of the Royal Society of London* A193(1032): 120–146.

Preisler, H. K., D. R. Brillinger, R. E. Burgan, and J. W. Benoit. 2004. "Probability based models for estimating wildfire risk." *International Journal of Wildland Fire* 13:133–142.

Preisler, H. K., and A. L. Westerling. 2007. "Statistical Model for Forecasting Monthly Large Wildfire Events in the Western United States." *Journal of Applied Meteorology and Climatology* 46(7): 1020–1030. DOI: 10.1175/JAM2513.1.

Ricotta, C., G. Avena, and M. Marchetti. 1999. "The flaming sandpile: Self-organized criticality and wildfires." *Ecological Modelling* 119:73–77.

Schlobohm, P., and J. Brain. 2002. *Gaining an Understanding of the National Fire Danger Rating System.* National Wildfire Coordinating Group Publication: NFES # 2665. www.nwcg.gov.

Schoenberg, F. P., R. Peng, and J. Woods. 2003. "On the distribution of wildfire sizes." *Environmetrics* 14:583–592.

Song, W., F. Weicheng, W. Binghong and Z. Jianjun. 2001. Self-organized criticality of forest fire in China. *Ecological Modelling* 145:61-68.

Stephenson, N. L. 1998. "Actual evapotranspiration and deficit: Biologically meaningful correlates of vegetation distribution across spatial scales." *J. Biogeog.* 25:855–870.

Strauss, D., L. Bednar, and R. Mees. 1989. "Do one percent of the forest fires cause ninety-nine percent of the damage?" *Forest Science* 35:319–328.

Swetnam, T. W., and J. L. Betancourt. 1998. "Mesoscale Disturbance and Ecological Response to Decadal Climatic Variability in the American Southwest." *Journal of Climate* 11:3128–3147.

Theobald, D. 2005. "Landscape patterns of exurban growth in the USA from 1980 to 2020." *Ecology and Society* 10(1): 32.

U.S. EPA. 2008. Preliminary Steps Towards Integrating Climate and Land Use (ICLUS): The Development of Land-Use Scenarios Consistent with Climate Change Emissions Storylines (External Review Draft). U.S. Environmental Protection Agency, Washington, D.C. EPA/600/R-08/076A.

Veblen, T. T., T. Kitzberger, and J. Donnegan. 2000. "Climatic and human influences on fire regimes in ponderosa pine forests in the Colorado Front Range." *Ecological Applications* 10: 1178–1195.

Verdin, K. L., and S. K. Greenlee. 1996. Development of continental scale digital elevation models and extraction of hydrographic features. In: *Proceedings, Third International Conference/Workshop on Integrating GIS and Environmental Modeling, Santa Fe, New Mexico, January 21–26, 1996.* National Center for Geographic Information and Analysis, Santa Barbara, California.

Westerling, A. L. In press. Climate Change Impacts on Wildfire. Chapter 12 in *Climate Change Science and Policy*. Schneider, Mastrandrea, and Rosencranz, Eds., Island Press. (English edition).

Westerling, A. L., T. J. Brown, A. Gershunov, D. R. Cayan, and M. D. Dettinger. 2003. "Climate and Wildfire in the Western United States." *Bulletin of the American Meteorological Society* 84(5): 595–604.

Westerling, A. L., and B. P. Bryant. 2008. "Climate Change and Wildfire in California." *Climatic Change* 87: s231-249. DOI:10.1007/s10584-007-9363-z.

Westerling, A. L., A. Gershunov, D. R. Cayan, and T. P. Barnett. 2002. "Long Lead Statistical Forecasts of Western U.S. Wildfire Area Burned." *International Journal of Wildland Fire* 11(3,4): 257–266. DOI: 10.1071/WF02009.

Westerling, A. L., H. G. Hidalgo, D. R. Cayan, T. W. Swetnam. 2006. "Warming and Earlier Spring Increases Western U.S. Forest Wildfire Activity." *Science* 313: 940–943. DOI:10.1126/science.1128834. Online supplement.

Zhang, Y.-H., M. J. Wooster, O. Tutubalina, and G. L. W. Perry. "Monthly burned area and forest fire carbon emission estimates for the Russian Federation from SPOT VGT." *Remote Sensing of Environment* 87:1–15.

7.0 Glossary

AET	actual evapotranspiration
BIA	Bureau of Indian Affairs
BLM	Bureau of Land Management
BOR	Bureau of Reclamation
CDF	California Department of Forestry and Fire Protection
CNRM	Centre National de Recherches Météorologiques
DOD	Department of Defense
FRA	federal protection responsibility area
FWS	Fisheries and Wildlife Service
GFDL	Geophysical Fluid Dynamics Laboratory
GIS	geographic information system
LDAS	Land Data Assimilation System
LRA	local protection responsibility area
NCAR PCM	National Center for Atmospheric Research Parallel Climate Model
NPS	U.S. Department of Interior's National Park Service
PCP	precipitation
PET	Potential Evapotranspiration
RH	relative humidity
SRA	state protection responsibility area
SRES	Special Report on Emissions Scenarios
SWE	snow-water equivalent
TMP	surface temperature

UMDvf   University of Maryland vegetation classification scheme with fractional
                 vegetation adjustment

USFS   U.S. Department of Agriculture's Forest Service

VIC   Variable Infiltration Capacity

Appendix A

Vegetation Allocation Method

Vegetation Allocation Method

A-1.1 Formalized Model Relating New Growth and Vegetation Cover

In our model for estimating fire probabilities, the fraction of each gridcell covered by vegetation plays an important role. In the limit of complete urbanization, it is clear that this variable is affected by encroaching human development, because a gridcell entirely covered by dense population would lack any sufficiently large vegetated space in which wildfires could exist. However, vegetation cover may be reduced by encroaching human development at intermediate scales as well, depending on how new growth is allocated. We model this allocation process as follows:

A given gridcell can be partitioned into the following disjoint areas, expressed as fractions of the gridcell they cover: Vegetation (V), urban (U), bare (B), agricultural (A), and water (W), with $V+U+B+A+W = 1$. These values exist for a baseline year, and when there is new urban growth with a footprint larger than the baseline urban fraction, it must be allocated to some combination of vegetation, bare, and agricultural land. To assess the range of impact that new growth may have on the vegetation fraction, we allot new growth in three different ways and consider the different impacts each method may have.

One is to maximize the wildfire-prone vegetation preserved, which is done by preferentially allotting new growth to the bare and agricultural areas before allotting any remaining growth to the vegetated areas:

$$V_{max} = V_0 - max(0, N-(A+B))$$

Where N is the new urban footprint requiring allocation—that is, the difference between the urban footprint in a given time versus the urban footprint in the base year. In this formulation, if there is sufficient agricultural and bare land to accommodate all new growth, the vegetation fraction is not reduced at all.

Another option is to reduce the vegetation fraction by as much as possible, assigning all new growth to the existing vegetated area:

$$V_{min} = max(0, V_0 - N)$$

These two allocation methods represent extreme bounds, and in reality growth will tend to be distributed among all three land types. As a middle option, we calculate the vegetation fraction assuming vegetated area is covered in direct proportion to how much area it occupies relative to agriculture and bare land:

$$V_{mid} = max(0, V_0 - N \, V_0/(A+N+V_0))$$

The results presented in this summary of our work as it presently stands are all for this middle option. When we extend our work to consider the A2 and B1 growth scenarios from ICLUS, we will incorporate these additional methods for estimating vegetation fraction.

A-1.2 Issues in Realizing the New Growth Measure

The above model is conceptually sound contingent on perfect knowledge of the relevant terms, but there exists great practical difficulty in obtaining a reasonable estimate for N, the area of new dense development requiring allocation. This difficulty arises from two issues: Uncertainty in the threshold density and spatial scale for defining what constitutes "urban" extent in different scenarios, and compatibility of the ICLUS scenarios with the with the LDAS urban and vegetation fractions.

For this analysis we assume that the 100m pixel level is the appropriate scale for defining urban density. Thus total urban extent within a gridcell is determined by determining what fraction of all 100m pixels within the gridcell have a household density greater than some threshold. The precise value of this threshold is not known to us and represents an uncertainty. The importance of this threshold differs depending on the allocation method used, and it may have zero marginal effect under many conditions when allocating to maximize vegetation preserved. For the middle and minimum vegetation allocations, its effect will depend on the distribution of pixel values within the gridcell.

The other issue is the compatibility between the LDAS land cover fractions, which are based on satellite imagery, and the urban fractions derived from the ICLUS scenarios. There is unfortunately poor correlation between the gridcell-level LDAS urban fractions and the urban fractions derived using our method in the base year 2000. In order to at least partially account for error this may introduce, we considered two thresholds, 147 and 1000 houses per square kilometer, chosen based on the ICLUS bounds for suburban housing density. However, with either threshold there remains a great deal of variation at the gridcell level, so that the ratio between scenario-based and LDAS-based urban fraction may vary significantly. For this analysis, the LDAS data produced a better fire probability model and was used to fit the model parameters to historical data, but for all base year and future model runs, the ICLUS vegetation fractions were used to drive model. The precise impact this has on fire probability estimates requires further investigation.